American Mineralogist, Volume 80, pages 873–877, 1995

Coordination of B in K_2O-SiO_2-B_2O_3-P_2O_5 glasses using B *K*-edge XANES

Dien Li,* G. M. Bancroft
Department of Chemistry, University of Western Ontario, London, Ontario N6A 5B7, Canada
M. E. Fleet
Department of Earth Sciences, University of Western Ontario, London, Ontario N6A 5B7, Canada
P. C. Hess
Department of Geological Science, Brown University, Providence, Rhode Island 02912, U.S.A.
Z. F. Yin
Department of Chemistry, University of Western Ontario, London, Ontario N6A 5B7, Canada

Abstract

High-resolution B *K*-edge X-ray absorption near-edge structure (XANES) spectra of K_2O-SiO_2-B_2O_3-P_2O_5 glasses are reported using synchrotron radiation. Two prominent features, peak a at about 194.0 eV and peak b at about 198.0 eV, are observed. On the basis of the qualitative MO diagrams of BO_3^{3-} and BO_4^{5-} clusters, peak a is assigned to the transition of B 1s electrons to the unoccupied B $2p_z$ (π^*) states for threefold-coordinated B ($^{[3]}$B), and peak b is assigned to the transition of B 1s electrons to the unoccupied B σ^* states for fourfold-coordinated B ($^{[4]}$B). B *K*-edge XANES spectroscopy is established as a method for "fingerprinting" $^{[3]}$B and $^{[4]}$B in borate and borosilicate minerals, glasses, and melts. Also, the relative proportions of $^{[4]}$B and $^{[3]}$B in the borosilicate glasses are determined from the integrated peak areas for $^{[3]}$B and $^{[4]}$B edge peaks and are shown to be generally in good agreement with recent ^{11}B MAS NMR measurements. However, the surface and near-surface structure of powder particles of perboric glasses containing P_2O_5 appears to have a lower proportion of $^{[3]}$B entities than the bulk.

Introduction

B is an important minor component in granites and pegmatites and plays important roles in the evolution of magma. For example, B lowers the solidus temperature of H_2O-saturated haplogranite (e.g., Chorlton and Martin, 1978; Pichavant, 1981), shifts phase boundaries in granitic systems (Chorlton and Martin, 1978; Pichavant, 1987), and decreases the viscosity of silicate melts (London, 1987). B^{3+} occurs in trigonal ($^{[3]}$B) and tetrahedral ($^{[4]}$B) coordinations in borate minerals (Christ and Clark, 1977) and glasses (Griscom, 1978; Gan et al., 1994).

The coordination structures of B in minerals and glasses have been investigated by Raman spectroscopy (Bunker et al., 1990; Gan et al., 1994; Konijnendijk and Stevels, 1976), ^{11}B MAS NMR spectroscopy (Bray, 1978; Bunker et al., 1990; Gan et al., 1994; Müller et al., 1993; Prabakar et al., 1990; Sen et al., 1994), B *K*-edge electron energy-loss near-edge structure (ELNES) (Brydson et al., 1988; Sauer et al., 1993; Garvie et al., personal communication), B $K\alpha$ X-ray emission (Luck and Urch, 1990), and structural modeling of glasses (Dell and Bray, 1983).

The B *K*-edge X-ray absorption near-edge structure (XANES) of molecular BF_3, BCl_3, and BBr_3 (Ishiguro et al., 1982) and BN polymorphs (Terminello et al., 1994) have been reported. The B *K*-edge XANES spectra of BF_3 and KBF_4 have been interpreted and the electronic structure and bonding of these compounds studied qualitatively on the basis of X_α-SW MO (Hallmeier et al., 1981; Schwarz et al., 1983), extended Hückel MO (Esposto et al., 1991), and MS-X_α MO calculations (Tossell, 1986; Vaughan and Tossell, 1973).

In this paper, we report high-resolution B *K*-edge XANES spectra of borosilicate glasses using synchrotron radiation. The B *K*-edge spectra are used as a structural "fingerprint" to determine the proportions of $^{[3]}$B and $^{[4]}$B in a series of peralkaline, subboric, and perboric glasses in the system K_2O-SiO_2-B_2O_3-P_2O_5, which were investigated recently by Raman and ^{11}B MAS NMR spectroscopy (Gan et al., 1994).

Experimental methods

Samples of borosilicate glasses in the system K_2O-SiO_2-B_2O_3-P_2O_5 (Table 1) were obtained from the study of Gan et al. (1994). The B *K*-edge XANES spectra were collected at room temperature using the Grasshopper beamline at the Canadian Synchrotron Radiation Facility (CSRF), University of Wisconsin (Bancroft, 1992). The radiation was monochromatized using a grating with 1800 grooves/mm, with energy resolution of about 0.2 eV at 200 eV.

* Present address: National Institute of Materials and Chemical Research, Tsukuba, Ibaraki 305, Japan.

0003–004X/95/0910–0873$02.00

TABLE 1. The [3]B and [4]B *K*-edge positions and calculated relative proportions of [3]B and [4]B in K_2O-SiO_2-B_2O_3-P_2O_5 glasses

Samples	B *K*-edge (±0.1 eV)		Area (arb. units) (±5%)		Abundance of B species* (%)				B_2O_3 (mol%)	K'**	P'**
					[3]B		[4]B				
	Peak a	Peak b	Peak a	Peak b	XANES	NMR	XANES	NMR			
B2	—	198.0	—	4.55	0	0	100	100	5.00	0.75	0
B3	—	198.0	—	3.91	0	0	100	100	4.92	0.75	0.26
B6	194.0	198.1	1.13	7.95	13	9	87	91	10.00	0.50	0
B7	194.0	198.1	1.82	7.83	19	17	81	83	9.83	0.50	0.15
B10	194.0	198.3	4.52	5.80	44	43	56	57	13.00	0.35	0
B11	194.0	198.3	4.09	5.52	43	48	57	52	12.78	0.35	0.12
B12	193.9	198.3	4.61	5.71	45	≥72	55	≤28	12.48	0.35	0.24

* Abundances of B calculated from ^{11}B MAS NMR spectra are cited from Gan et al. (1994).
** $K' = K_2O/(K_2O + B_2O_3)$; $P' = P_2O_5/(P_2O_5 + B_2O_3)$.

The B *K*-edge XANES spectra were recorded by total electron yield (TEY) as a function of photon energy from 180 to 220 eV. For the B *K*-edge measurements, powder samples (≤5 μm) were spread uniformly on Cu tape on a sample holder and transferred into the experimental chamber, which was maintained at a vacuum of 10^{-8} torr during the measurements. All samples were prepared in a similar manner to minimize the effect of sample thickness and particle size on the relative intensity of absorption features. Three measurements were made for each sample. The spectrum for each measurement was normalized by I/I_0, where I is TEY intensity, and I_0 is the intensity of the photon flux. The raw spectrum for each sample investigated was averaged from the normalized spectra for the three measurements and smoothed. A linear preedge background was removed from each spectrum. All spectra were calibrated using the edge peak of B_2O_3 at 194.0 eV.

RESULTS AND INTERPRETATION

Figure 1 shows the B *K*-edge XANES spectra of crystalline B_2O_3 and BPO_4. These are raw spectra without smoothing, and the interval between two data points is 0.05 eV. The qualitative MO diagrams for BO_3^{3-} and BO_4^{5-} clusters in the inset are modified from X_α-SW MO calculations of BF_3 and KBF_4 (Schwarz et al., 1983). B is threefold coordinated with O in B_2O_3. BPO_4 is isostructural to cristobalite, which is confirmed by powder X-ray diffraction, and B is fourfold coordinated with O. A sharp peak a at about 194.0 eV and a broad band c at about 202 eV are observed in the B *K*-edge spectrum of B_2O_3. The full width at half maximum (FWHM) of peak a is 0.60 eV. For BPO_4, the first prominent peak b is at about 198.0 eV, with a FWHM of 1.35 eV; a second broad peak c' is at about 203 eV.

In previous studies (e.g., Li et al., 1994), we have interpreted the *K*- and *L*-edge features of third-period elements (Al, Si, P, and S) to represent the transitions of core (1s or 2p) electrons to the unoccupied density of states (DOS) or the antibonding states. The present B *K*-edge features appear to have a similar origin. Qualitative interpretations of these spectra are based on comparison with B *K*-edge XANES, ELNES (Brydson et al., 1988; Sauer et al., 1993; Garvie et al., personal communication), and MO calculations (Esposto et al., 1991; Hallmeier et al., 1981; Schwarz et al., 1983; Tossell, 1986; Vaughan and Tossell, 1973) of model B compounds containing [3]B, [4]B, or both. As shown in Figure 1, for B_2O_3, peak a is attributed uniquely to [3]B and is further assigned to the transition of B 1s electrons to the unoccupied B $2p_z$ (π^*) states for threefold-coordinated B with O. The broad feature c is assigned to the transitions of B 1s electrons to the unoccupied B σ^* states. A very weak feature between peaks a and c may be assigned to the transition of B 1s electrons to the empty B 3p states. In the B *K*-edge spectrum of BPO_4, peak b is uniquely attributed to [4]B and is further assigned to the transition of B 1s electrons to the unoccupied B σ^* states for fourfold-coordinated B with O. The broad peak c' may be due to the transitions of B 1s electrons to the unoccupied σ^* states of [4]B, and it may have additional contribution from the multiple-scattering effect.

Figure 2 shows the B *K*-edge XANES spectra of the K_2O-SiO_2-B_2O_3-P_2O_5 glass samples investigated. The energy positions of peaks a and b for these borosilicate glasses are given in Table 1; the reading error is about ±0.1 eV. Again, peak a is assigned to transitions of B 1s electrons to the unoccupied B $2p_z$ (π^*) for [3]B, and peak b is assigned to transitions of B 1s electrons to the unoccupied B σ^* for [4]B. Peak a for [3]B is at about 194.0 eV and does not appear to shift among the labeled samples investigated to date because the B $2p_z$ state projects normal to the trigonal bonding plane and does not experience significant steric interference. Peak b for [4]B is at about 198.0 eV and shows evidence of both complexity and shifts from samples B2 to B12 (Fig. 2). Thus, the first unoccupied state for [4]B is about 4 eV above that for [3]B, and B *K*-edge XANES spectra can be used as an excellent structural "fingerprint" for distinguishing [3]B and [4]B.

The B *K*-edge XANES spectra of the K_2O-SiO_2-B_2O_3-P_2O_5 glasses were fitted to estimate semiquantitatively the relative proportions of [3]B and [4]B in glasses containing B in both trigonal and tetrahedral sites. Crystalline B_2O_3, which contains [3]B only, was used as the model compound to separate the features attributed to [3]B and [4]B. Peak a in the B *K*-edge spectrum of B_2O_3 was nor-

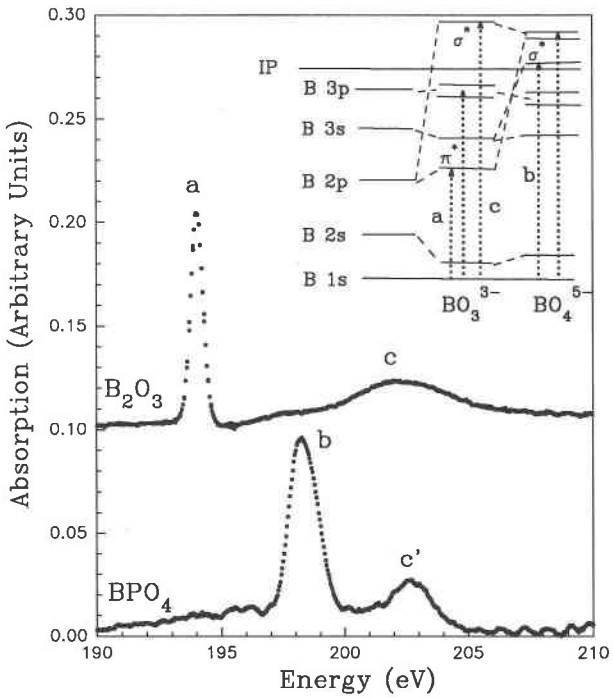

Fig. 1. B *K*-edge XANES spectra of B_2O_3, containing only [3]B, and BPO_4, containing only [4]B. These spectra are raw data without smoothing. A peak a in the BPO_4 spectrum, which may be due to surface damage of the sample, has been removed. Qualitative MO diagrams for BO_3^{3-} and BO_4^{5-} (inset) are modified from X_α-SW MO calculations of BF_3 and KBF_4 molecules (Schwarz et al., 1983). IP is ionization potential.

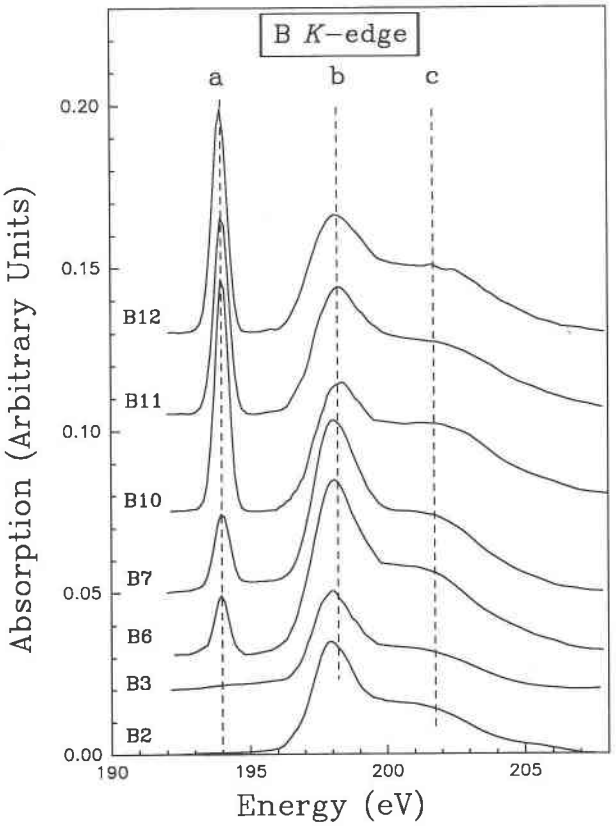

Fig. 2. B *K*-edge XANES spectra of K_2O-SiO_2-B_2O_3-P_2O_5 glasses.

malized to the height of a peak a of each glass spectrum, and so the difference spectrum between the sample and B_2O_3 represents the features for [4]B. The latter spectrum was fitted into a Gausian peak b and a broad peak c′ (Fig. 3). The areas (arbitrary units) of peaks a and b, which are attributed solely to [3]B and [4]B, respectively, are given in Table 1 and have been used directly to calculate the relative abundances of [3]B and [4]B in the glass samples (Table 1). The contents of $[3]B_2O_3$ and $[4]B_2O_3$ entities in the glasses can also be calculated using the total content of B_2O_3 determined by EMPA (Table 1).

Discussion

The ^{11}B MAS NMR (Gan et al., 1994) and B *K*-edge ELNES (Garvie et al., personal communication; Sauer et al., 1993) techniques have been used to estimate the relative abundances of [3]B and [4]B in minerals and glasses containing both [3]B and [4]B. Similarly, we have used the B *K*-edge XANES spectra to determine the relative abundances of [3]B and [4]B species in the present borosilicate glasses by relating the peak areas to the concentration of the B species (Table 1). Figure 4 compares the abundance of [3]B in peralkaline, subboric, and perboric glasses in the K_2O-SiO_2-B_2O_3-P_2O_5 system, derived from B *K*-edge XANES spectra in this work and from ^{11}B MAS NMR spectra in Gan et al. (1994). The abundances of [3]B species from these two techniques are generally comparable, with the single exception of sample B12. The proportion of [3]B increases with increase in total content (mole percent) of B_2O_3 and with decrease in the content of K_2O from peralkaline ($K' = 0.75$) to subboric ($K' = 0.5$) and perboric ($K' = 0.35$) glasses, in agreement with ^{11}B MAS NMR results (Gan et al., 1994). Thus, both B *K*-edge XANES and ^{11}B MAS NMR techniques not only ambiguously distinguish [3]B and [4]B but also are in excellent agreement on the proportions of [3]B and [4]B in the peralkaline and subboric glasses (see Fig. 4). However, B *K*-edge XANES indicates a constant proportion of [3]B in the perboric glasses, more or less independent of the content of P_2O_5 (Table 1).

The combined Raman and ^{11}B and ^{31}P MAS NMR study of Gan et al. (1994) on the present glass samples showed that P_2O_5 has a significant effect on the redistribution of O and alkali cations among different structural units in K_2O-SiO_2-B_2O_3-P_2O_5 glasses. The effect of P_2O_5 is manifested by a shift in the coordination of B from [4]B to [3]B in the perboric and subboric glasses and by polymerization of silicate species from Q^3 to Q^4 in the peralkaline glasses. The model of Dell and Bray (1983) for potassium borosilicate glasses assumed that alkali-borate binary structural units are retained in alkali-borosilicate ternary glasses for $K' \leq 0.35$, but Gan et al. (1994) showed

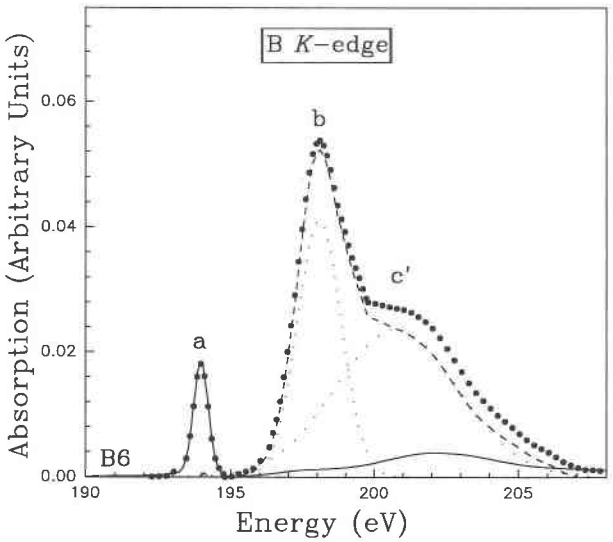

Fig. 3. Curve fitting of the B *K*-edge XANES spectrum of sample B6. The heavy dotted line is the experimental spectrum. Peak a in the B *K*-edge spectrum of crystal B_2O_3 (containing only [3]B) was normalized to the height of peak a of sample B6; thus, the solid line is the contribution of [3]B, and the difference spectrum between the sample and crystalline B_2O_3 represents the features for [4]B (dashed line). The features for [4]B were fitted into a Gaussian peak b and a broad peak c′ (light dotted lines). The areas (arbitrary units) of peaks a and b, which are attributed to [3]B and [4]B, respectively, are given in Table 1.

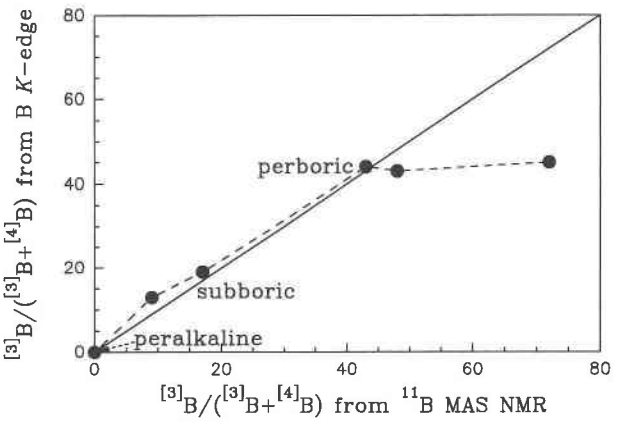

Fig. 4. Comparison of relative abundances of [3]B species derived from B *K*-edge XANES (this study) and ^{11}B MAS NMR spectra (Gan et al., 1994) of K_2O-SiO_2-B_2O_3-P_2O_5 glasses.

that the addition of SiO_2 not only dilutes but also interacts with alkali-borate species in this concentration range.

The present B *K*-edge XANES study does not add to this detailed understanding of the bulk structure of the K_2O-SiO_2-B_2O_3-P_2O_5 glasses. Peak a, attributed to [3]B (see Fig. 2), is narrow but does not appear to be sensitive to stereochemical environment. The ^{11}B MAS NMR feature for [3]B is a group of broad peaks centered at 9 ppm and assigned by Gan et al. (1994) to unaveraged second-order quadrupolar effects and asymmetric and symmetric [3]B groups. However, as noted above, the B *K*-edge XANES spectra do show evidence of the two distinct [4]B environments (B with B NNN and B with Si NNN), although these two features are not resolved completely. Peak b (for [4]B) in the B *K*-edge spectra shows a small shift to higher energy and progressive broadening (Fig. 2) in the sequence of peralkaline, subboric, and perboric glasses (from sample B2 to sample B12). These results indicate that both the polymerization of the glasses and the proportion of B species with B NNN increase in the same sequence, in agreement with the ^{11}B MAS NMR spectra, in which the [4]B entities are represented by unresolved peaks centered at −2 and 0 ppm.

The discrepancy between this work and Gan et al. (1994) for the proportion of [3]B in sample B12 (and B1112) may be attributable to curve fitting of the ^{11}B MAS NMR spectra, but surface and near-surface reorganization of the glass structure during either sample preparation or initial irradiation is the most likely explanation. We have recently experienced some spurious enhancement of the [3]B peak in subsequent B *K*-edge XANES work, which may be attributable to the surface or near-surface damage of samples. TEY is much more surface sensitive than other collection modes of XANES spectra, and it is very sensitive to the surface and near-surface structure to a depth of about 70 Å from the surface at the B *K*-edge region. However, the fluorescence-yield detection mode provides structural information of samples up to a depth of 1000 Å from the surface at the B *K*-edge region. We anticipate that fluorescence-yield B *K*-edge spectroscopy will prove to be a more satisfactory method for studying the bulk structure of these glasses (Kasrai et al., 1993). However, the B *K*-edge XANES spectra collected by TEY may have yielded unexpected insight into the surface and near-surface structure of powder particles of these potassium borosilicate–phosphate glasses. For example, addition of P_2O_5 to perboric glasses may inhibit the formation of [3]B entities in the surface of quenched glass. This phenomenon could have significance for the chemical stability and physical properties of borosilicate glass products.

B *K*-edge ELNES spectroscopy, with the help of improved resolution, is indeed a powerful method for identifying the entities of [3]B and [4]B in minerals and glasses. However, the high-energy electron beam may damage the surface of samples and transform a small amount of [4]B into [3]B (Brydson et al., 1988; Sauer et al., 1993). For samples containing only [4]B, the proportion of [3]B increases with increase in exposure to the electron beam (Sauer et al., 1993). Sauer et al. (1993) and Garvie et al. (personal communication) also used ELNES spectroscopy to determine the proportions of [3]B and [4]B in borate minerals. However, more care must be taken when ELNES spectroscopy is used for quantitative analysis of [3]B and [4]B because of possible surface damage of samples and transformation of [4]B into [3]B by the high-energy electron beam.

Synchrotron radiation B *K*-edge XANES spectroscopy

has many advantages for the quantification of [3]B and [4]B. Sample preparation is very simple, and the use of synchrotron radiation permits rapid acquisition of B *K*-edge XANES spectra. The prominent features attributed to [3]B and [4]B are well separated by about 4 eV, as in the ELNES spectrum, and, in particular, peak a, assigned to [3]B, is very sharp. B *K*-edge XANES spectroscopy appears to overcome some disadvantages of ^{11}B MAS NMR and B *K*-edge ELNES spectroscopy in quantification of the local structure of B. By comparing the quantification techniques used by Sauer et al. (1993) with those developed here, our technique gave abundances of [3]B and [4]B in these glasses that are in better agreement with the ^{11}B MAS NMR results (Gan et al., 1994). The accuracy of the XANES technique is difficult to evaluate, but the proportions of [3]B and [4]B entities are estimated to be within ±10%. The variation in sample preparation and the slightly different cross sections of [3]B and [4]B may contribute to the error.

Acknowledgments

This work was supported by NSERC. We thank K.H. Tan, Canadian Synchrotron Radiation Facilities (CSRF), and the staff at the Synchrotron Radiation Center (SRC), University of Wisconsin, for their technical assistance. The National Science Foundation (NSF) is thanked for its support of the SRC.

References cited

Bancroft, G.M. (1992) New developments in far UV, soft X-ray research at the Canadian Synchrotron Radiation Facilities. Canadian Chemical News, 44, 15–22.

Bray, P.J. (1978) NMR studies of borates. In L.D. Pye, V.D. Fréchette, and N.J. Kreidel, Eds., Borate glasses: Structure, properties, applications. Materials Science Research, 12, 321–352.

Brydson, R., Williams, B.G., Engel, W., Lindner, T., Muhler, M., Schlögl, R., Zeitler, E., and Thomas, J.M. (1988) Electron energy-loss spectroscopy and the crystal chemistry of rhodizite. Journal of the Chemical Society, Faraday Transaction I, 84, 631–646.

Bunker, B.C., Tallant, D.R., Kirkpatrick, R.J., and Turner, G.L. (1990) Multinuclear magnetic resonance and Raman investigation of sodium borosilicate glass structures. Physics and Chemistry of Glasses, 29, 106–120.

Chorlton, L.B., and Martin, R.F. (1978) The effect of boron on the granite solidus. Canadian Mineralogist, 16, 239–244.

Christ, C.L., and Clark, J.R. (1977) A crystal-chemical classification of borate structures with emphasis on hydrated borates. Physics and Chemistry of Minerals, 2, 59–87.

Dell, W.J., and Bray, P.J. (1983) ^{11}B NMR studies and structural modelling of Na_2O-B_2O_3-SiO_2 glasses of high soda content. Journal of Non-Crystalline Solids, 58, 1–16.

Esposto, F.J., Aebi, P., Tyliszczak, T., Hitchcock, A.P., Kasrai, M., Bozek, J.D., Jackman, T.E., and Rolfe, S.R. (1991) Boron K-shell spectroscopy of boron-doped silicon. Journal of Vacuum Science and Technology, A9, 1663–1669.

Gan, H., Hess, P.C., and Kirkpatrick, R.J. (1994) Phosphorus and boron speciation in K_2O-B_2O_3-SiO_2-P_2O_5 glasses. Geochimica et Cosmochimica Acta, 58, 4633–4647.

Griscom, D.L. (1978) Borate glass structure. In L.D. Pye, V.D. Fréchette, and N.J. Kreidel, Eds., Borate glasses: Structure, properties, applications. Materials Science Research, 12, 11–138.

Hallmeier, K.H., Szargan, R., Meisel, A., Hartmann, E., Gluskin, E.S. (1981) Investigation of core-excited quantum, yield spectra of high-symmetric boron compounds. Spectrochimica Acta, 37A, 1049–1053.

Ishiguro, E., Iwata, S., Suzuki, Y., Mikuni, A., and Sasaki, T. (1982) The boron *K* photoabsorption spectra of BF_3, BCl_3 and BBr_3. Journal of Physics B: Atomic and Molecular Physics, 15, 1841–1854.

Kasrai, M., Yin, Z.F., Bancroft, G.M., and Tan, K.H. (1993) X-ray fluorescence measurements of X-ray absorption near edge structure at the Si, P and S *L*-edges. Journal of Vacuum Science and Technology, A11, 2694–2699.

Konijnendijk, W.L., and Stevels, J.M. (1976) The structure of borosilicate glasses studied by Raman scattering. Journal of Non-Crystalline Solids, 20, 193–224.

Li, D., Bancroft, G.M., Kasrai, M., Fleet, M.E., Secco, R.A., Feng, X.H., Tan, K.H., and Yang, B.X. (1994) X-ray absorption spectroscopy of silicon dioxide (SiO_2) polymorphs: The structural characterization of opal. American Mineralogist, 79, 622–632.

London, D. (1987) Internal differentiation of rare element pegmatites: Effects of boron, phosphorus and fluorine. Geochimica et Cosmochimica Acta, 51, 403–420.

Luck, S., and Urch, D.S. (1990) Boron *K* alpha X-ray emission and the electronic structure of boron compounds: Coordination and resonance emission. Physica Scripta, 41, 970–972.

Müller, D., Grimmer, A.R., Timper, U., Heller, G., and Shakibaie-Moghadam, M. (1993) ^{11}B-MAS-NMR-untersuchungen zur anionenstruktur von boraten. Zeitschrift für Anorganische und Allgemeine Chemie, 619, 1262–1268.

Pichavant, M. (1981) An experimental study of the effect of boron on a water saturated haplogranite at 1 kbar vapour pressure. Contributions to Mineralogy and Petrology, 76, 430–439.

——— (1987) Effects of B and H_2O on liquidus phase relations in the haplogranite system at 1 kbar. American Mineralogist, 72, 1056–1070.

Prabakar, S., Rao, K.J., and Rao, C.N.R. (1990) ^{11}B NMR spectra and structure of boric oxide and alkali borate glasses. Proceedings of the Royal Society of London, A429, 1–15.

Sauer, H., Brydson, R., Rowley, P.N., Engel, W., and Thomas, J.M. (1993) Determination of coordinations and coordination-specific site occupancies by electron energy-loss spectroscopy: An investigation of boron-oxygen compounds. Ultramicroscopy, 49, 198–209.

Schwarz, W.H.E., Mensching, L., Hallmeier, K.H., and Szargon, R. (1983) *K*-shell excitations of BF_3, CF_4 and MBF_4 compounds. Chemical Physics, 82, 57–65.

Sen, S., Stebbins, J.F., Hemming, N.G., and Ghosh, B. (1994) Coordination environments of B impurities in calcite and aragonite polymorphs: A ^{11}B MAS NMR study. American Mineralogist, 79, 819–825.

Terminello, L.J., Chaiken, A., Lapiano-Smith, D.A., and Sato, T. (1994) Morphology and bonding measured from boron-nitride powders and films using near-edge X-ray absorption fine structure. Journal of Vacuum Science and Technology, A12, 2462–2466.

Tossell, J.A. (1986) Studies of unoccupied molecular orbitals of the B-O bond by molecular orbital calculations, X-ray absorption near edge, electron transmission, and NMR spectroscopy. American Mineralogist, 71, 1170–1177.

Vaughan, D.J., and Tossell, J.A. (1973) Molecular orbital calculations on beryllium and boron oxyanions: Interpretation of X-ray emission, ESCA, and NQR spectra and of the geochemistry of beryllium and boron. American Mineralogist, 58, 765–770.

Manuscript received January 27, 1995
Manuscript accepted May 9, 1995